Stacking Models of Vesicles and Compact Clusters

Thomas Prellberg[1,2] and Aleksander L. Owczarek[1]

We investigate three simple lattice models of two dimensional vesicles. These models differ in their behavior from the universality class of partially convex polygons, which has been recently established. They do not have the tricritical scaling of those models, and furthermore display a surprising feature: their (perimeter) free energy is discontinuous with an isolated value at zero pressure. We give the full asymptotic descriptions of the generating functions in area and perimeter variables from the q-series solutions and obtain the scaling functions where applicable.

1. INTRODUCTION

Stacking models of compact clusterings of molecules were first considered physically as descriptions of the form of crystal surfaces[1] in two dimensions. Mathematically they are intimately connected to the partitioning of integers[2-5] and are prototypical objects for the study of geometric phase transitions.[6,7] Recently, the enumeration of lattice polygon configurations by area and perimeter has been of interest in the understanding of the shapes of flexible vesicles.[8] The generic structure of the resulting phase diagram contains a point where, mathematically, tricritical scaling is observed. The analysis of partially convex subsets of self-avoiding polygons[9,10] has confirmed this behavior while allowing a fairly complete mathematical description. These partially convex polygons form a universality class with the same crossover exponent as expected in the unrestricted problem. The

---

[1] Department of Mathematics, University of Melbourne, Parkville, Victoria 3052, Australia. E-mail: prel,aleks@mundoe.maths.mu.oz.au.

[2] Present address: Mathematics Institute, University of Oslo, Blindern, N-0316 Oslo, Norway.
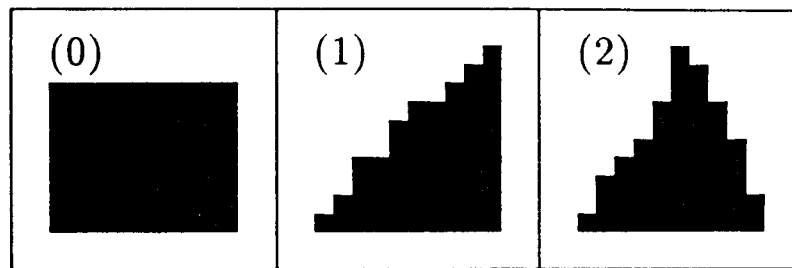
Fig. 1. Typical configurations of the stacking vesicle models: (0) rectangles; (1) Ferrers diagrams; and (2) stacks.

stacking models can also be extended to describe vesicles. Solutions for the full area–perimeter generating functions necessary for these descriptions have been calculated by several groups[5, 11, 12],[3] or have been known under other guises.[3] Here we are interested in the asymptotics of these solutions. We also consider the semicontinuous versions of the models, which are shown to have the same asymptotic behavior, where applicable. This allows us to determine the phase diagrams of the stacking models and extract their scaling functions. We explicitly demonstrate that the tricritical forms are absent in these models and catalog the nature of each phase transition mathematically. While a few of the results contained in this work were known previously, we provide a self-contained discussion for reasons of clarity.

This work is concerned with three models (see Fig. 1). The first is trivial (at least in definition): simple rectangles. The other two are Ferrers diagrams[2, 14, 1, 3],[4] and stacks.[1, 15, 16] This hierarchy is of pedagogical value, as we can consider the effect of the successive addition of complexity. In contrast to this, we have found a unity to the mathematical description of these models. For both reasons it is natural to present all three models together.

For each of these models, we define the generating function as follows. Let $c_m^{n_x, n_y}$ be the number of polygons with $2n_x$ horizontal steps and $2n_y$ vertical steps which enclose an area of size m. (Clearly the numbers of horizontal and vertical steps are even.) We then define the polygon generating function $G(x, y, q)$ to be

$$G(x, y, q) = \sum c_m^{n_x, n_y} x^{n_x} y^{n_y} q^m \qquad (1.1)$$

---

[3] M. Bousquet-Mélou, M. Delest, E. J. Janse van Rensburg, M. C. Tesi, S. Whittington, and the present authors all have recently calculated the area–perimeter generating function for stacks.

[4] A brief summary of some of the results for this model was announced in ref. 13.

This generating function allows us to consider the fixed area $A_m(x, y)$ and fixed perimeter $P_n(q)$ partition functions,

$$A_m(x, y) = \sum_n c_m^{n_x, n_y} x^{n_x} y^{n_y} \quad \text{and} \quad P_n(q) = \sum_m c_m^n q^m \tag{1.2}$$

where c_m^n is the number of polygons with a $2n$-step perimeter that encloses an area of size m, since

$$G(x, y, q) = \sum_m A_m(x, y) q^m \tag{1.3}$$

and

$$G(z, q) \equiv G(z, z, q) = \sum_n P_n(q) z^n \tag{1.4}$$

Let us first consider the generating function $G(z, z, q)$ as a power series in z with coefficients $P_n(q)$. Its radius of convergence $z_c(q)$ is given by

$$z_c(q) = \lim_{n \to \infty} P_n(q)^{-1/n} \tag{1.5}$$

Hence, the radius of convergence in z is simply related to the (reduced) perimeter free energy $f(q)$ as $z_c(q) = \exp(f(q))$. In other vesicle models[8, 9] the dependence of the radius of convergence $z_c(q)$ on q is expected to be of the generic form shown in Fig. 2(a). The function $z_c(q)$ is an analytic
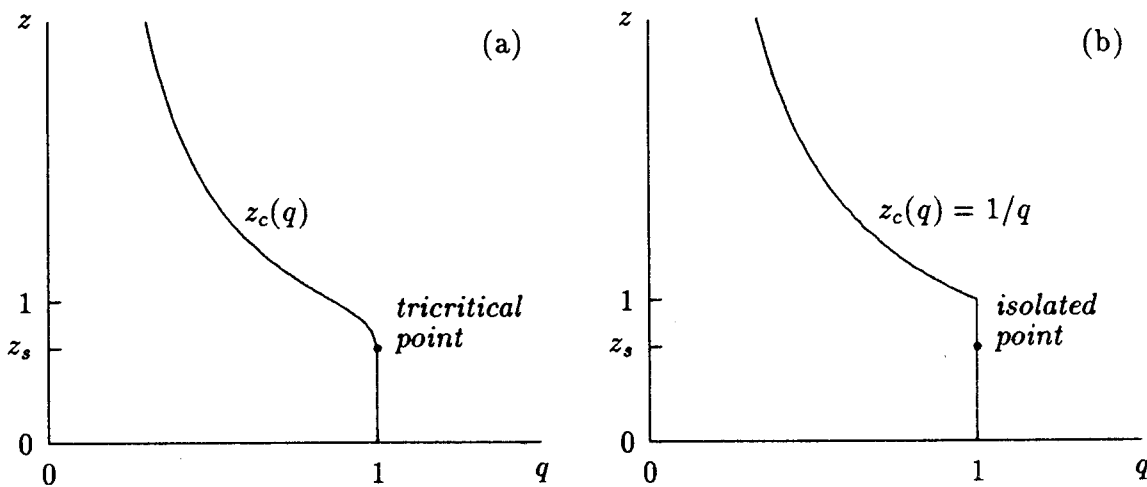

Fig. 2. The schematic form of the locus of singularities of the area–perimeter generating functions for vesicle models: (a) generic vesicle model; (b) stacks and Ferrers diagrams. Considered as a function of z, it is a continuous function, while considered as a function of q, it has a jump discontinuity at $q = 1$ in both cases. Furthermore, in case (b) there is an isolated point $z_c(1)$ at $q = 1$; in case (a), $\lim_{q \to 1^-} z_c(q) = z_c(1)$.

function of q for $0 < q < 1$ with a jump to $z_c = 0$ for $q > 1$. In the more complex polygon models such as staircase polygons, one finds that $z_s = z_c(1)$ and $\lim_{q \to 1^-} z_c(q)$ coincide, and that the scaling behavior around the point $(z = z_s, q = 1)$ is tricritical (see below).

However, a study of the simpler models revealed that this need not be the case.[5] In fact, we will show below that for stack polygons and Ferrers diagrams

$$1 = \lim_{q \to 1^-} z_c(q) < z_c(1) < \lim_{q \to 1^+} z_c(q) = 0 \tag{1.6}$$

that is, there is a jump discontinuity in $z_c(q)$ at $q = 1$ with an isolated point at $z_s = z_c(1)$ (that is, a *zeroth-order* phase transition), and we will get the behavior depicted in Fig. 2(b).[6] We now have different scaling behavior in the generating function around $(1, 1)$ and $(1, z_s)$. (In the semicontinuous models we define later, it is usual to consider the partition functions of either fixed horizontal or vertical perimeter; this gives the same generic picture as described above.) Because of the isolated point/jump discontinuity in $z_c(q)$ there is no crossover scaling form (see below) for $P_n(q)$ around $q = 1$ for large n.

One can also consider the radius of convergence of the generating function in the variable q. This is defined as

$$q_c(x, y) = \lim_{m \to \infty} A_m(x, y)^{-1/m} \tag{1.7}$$

Let us consider putting $z = x = y$ and then vary z (alternately one could fix x and vary $z = y$). In the stacking models we will show that there are three types of behavior. For $z > 1$ the generating function has a pole at its radius of convergence $q_c(z)$. As z approaches 1 we have $q_c(z) \to 1$. For $z_s < z \leqslant 1$ the generating function has a divergent essential singularity:

$$G(z, q) \sim A(1 - q)^\delta\, e^{B/(1 - q)} \tag{1.8}$$

and the power δ takes on different values for $z = 1$ and $z < 1$. For $z = z_s$ there is a power-law singularity in the generating function. Finally, for $z < z_s$ the generating function converges to a constant and, moreover, has a (convergent) essential singularity which can be expressed as an asymptotic expansion.

The behavior of the generating function on approaching the radius of convergence gives information on the asymptotic behavior of the partition functions for large sizes. For example, the behavior of $G(x, y, q)$,

[5] This was pointed out to us by E. J. Janse van Rensburg and S. Whittington.

[6] This behavior does not contradict the usual convexity property of the free energy, since it is unbounded for $q > 1$.

considered as a polynomial in q, near the radius of convergence $q_c(x, y)$ gives the asymptotic behavior of $A_m(x, y)$ for large m. Hence, the different asymptotic behaviors of the generating function described in the previous paragraph can be translated to behaviors for the partition function. When the generating function behaves as

$$G(z, q) \sim \frac{A}{(q_c - q)^\gamma} \qquad (1.9)$$

then

$$A_m(z) \sim \frac{A q_c^{-\gamma}}{\Gamma(\gamma)} q_c^{-m} m^{\gamma - 1} \qquad (1.10)$$

If the generating function has the divergent essential singularity behavior described in Eq. (1.8), then

$$A_m(z) \sim \frac{A}{(4\pi)^{1/2} B^{(2\delta + 5)/4}} e^{2(Bm)^{1/2}} m^{-(2\delta + 3)/4} \qquad (1.11)$$

The convergent essential singularity will be seen later to imply that

$$A_m(z) \sim C e^{-b(m)^{1/2}} m^d \qquad (1.12)$$

with $b > 0$.

For the partially convex models such as staircase polygons the tri-critical behavior mentioned is defined as follows. Around the tricritical point ($z = z_s$, $q = 1$) the two-variable generating function scaled by its behavior on approaching $q = 1$ fixed at $z = z_s$ is asymptotically equal to a function of one variable (known as the scaling variable). This one variable is a product of powers of the distances to the tricritical point in the two directions. Mathematically, for $z \to z_s$ and $q \to 1$ we expect

$$(1 - q)^{\gamma_s} G(z, q) \sim \mathscr{G}((1 - q)^{-\phi} (z - z_s)) \qquad (1.13)$$

where $G(z_s, q) \sim A(1 - q)^{-\gamma_s}$ and ϕ is the crossover exponent. Moreover, the (tricritical) scaling function $\mathscr{G}(\lambda)$ describes the crossover between the power-law behavior for $z > z_s$ through the scaling region where there is a different power-law behavior (characterised by the exponent γ_s) to a convergent essential singularity for $z < z_s$. The crossover exponent is related to the ratio of exponents of the singular (power-law) behavior of the generating function in the limits ($z = z_s$, $q \to 1^-$) and ($z \to z_s^-$, $q = 1$) [that is, if $G(z_s, q) \sim A(1 - q)^{-\overline{\gamma}_s}$ as $q \to 1^-$, then $\phi = \gamma_s / \overline{\gamma}_s$]. This behavior defines a tricritical point mathematically. [We are using the (limited) physical definition of a tricritical point as the (critical) meeting of a line of critical points smoothly with a line of first-order transitions.]

It will be seen in the stacking models that there is no tricritical point. However, one can still ask whether there is some form of crossover scaling around the points $(z = 1, \ q = 1)$ and $(z = z_s, \ q = 1)$. We shall explore this question and show that there is a scaling function around the second point for the generating function (and for the area partition function around $z = z_s$ for large m).

2. THE GENERATING FUNCTIONS

2.1. Discrete Models

We can derive the area–perimeter generating function for each of the models by using an inflation process[11, 10, 17]: the height of the polygon is increased by one lattice spacing and concatenated with rows of height one. This process generates all polygons of height larger than one, so that we have to add explicitly columns of height one after inflation in order to get all the polygons (see Fig. 3). Written as a functional equation, we have

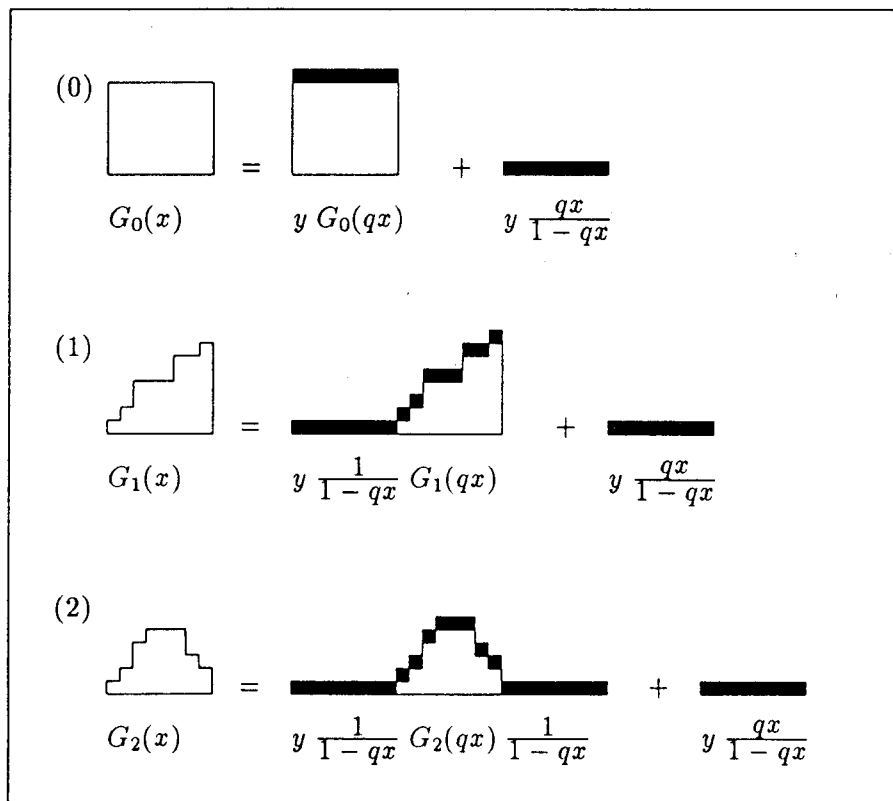$$G_s(x, y, q) = \frac{y}{(1 - qx)^s} G_s(qx, y, q) + \frac{yqx}{1 - qx} \tag{2.1}$$

Fig. 3. Diagrammatic form of the functional equations for (0) rectangles, (1) Ferrers diagrams, and (2) stacks.

where the parameter s is equal to the number of concatenated rows. We identify rectangles with $s = 0$, Ferrers diagrams with $s = 1$, and stacks with $s = 2$. Solving Eq. (2.1) by iteration leads to

$$G_s(x, y, q) = \sum_{n=1}^{\infty} \frac{x(yq)^n}{(xq; q)_{n-1}^s (1 - xq^n)}$$ (2.2)

where we have used the q-product notation

$$(t; q)_n = \prod_{m=0}^{n-1} (1 - tq^m)$$ (2.3)

For rectangles and Ferrers diagrams we can present q-series expansions that directly show the symmetry of the models:

$$G_0(x, y, q) = \sum_{n=1}^{\infty} \frac{(xy)^n q^{n^2}(1 - q^{2n}xy)}{(1 - q^n x)(1 - q^n y)}$$

$$G_1(x, y, q) = \sum_{n=1}^{\infty} \frac{(xy)^n q^{n^2}}{(qx; q)_n (qy; q)_n}$$ (2.4)

Also, we have three special cases in which we can evaluate the generating functions further. First, $G_1(1, y, q)$ is simply the series expansion for the q-exponential, so that

$$G_1(1, y, q) = \frac{1}{(yq; q)_\infty} - 1$$ (2.5)

Second, if we consider the area-only generating function for stacks,[15] we get

$$G_2(1, 1, q) = \frac{1}{(q; q)_\infty^2} \sum_{m=0}^{\infty} (-1)^m q^{\binom{m}{2}}$$ (2.6)

This result can be derived using the transformation

$$\sum_{n=1}^{\infty} \frac{q^n}{(q; q)_n} (q^n, q)_\infty = \sum_{n=1}^{\infty} \frac{q^n}{(q; q)_n} \sum_{m=0}^{\infty} \frac{q^{\binom{m}{2}}(-q^n)^m}{(q; q)_m}$$

$$= \sum_{m=0}^{\infty} \frac{(-1)^m q^{\binom{m}{2}}}{(q; q)_m} \sum_{n=1}^{\infty} \frac{(q^{1+m})^n}{(q; q)_n}$$

$$= \sum_{m=0}^{\infty} \frac{(-1)^m q^{\binom{m}{2}}}{(q; q)_m} \left(\frac{1}{(q^{1+m}; q)_\infty} - 1 \right)$$

$$= \frac{1}{(q; q)_\infty} \sum_{m=0}^{\infty} (-1)^m q^{\binom{m}{2}}$$ (2.7)

Finally, for $q = 1$, one gets the perimeter-generating functions

$$G_s(x, y, 1) = \frac{xy(1-x)^{s-1}}{(1-x)^s - y} \tag{2.8}$$

2.2. Semicontinuous Models

One can consider taking the semicontinuous limit of the models, either in a horizontal or vertical direction, by introducing a lattice spacing a and considering the limit $a \to 0$. For convenience, we introduce the notation

$$\sigma = -\log x, \qquad \tau = -\log y, \qquad \varepsilon = -\log q \tag{2.9}$$

One can solve the horizontal limit problem directly via integral equation methods.[18,9] This yields the solutions

$$G_s^{(h)}(x, y, q) = \sum_{n=1}^{\infty} \frac{y^n}{\prod_{m=1}^{n-1} (\sigma + m\varepsilon)^s (\sigma + n\varepsilon)}$$

$$= \sum_{n=1}^{\infty} \frac{\Gamma^s(\sigma/\varepsilon + 1)}{\Gamma^s(\sigma/\varepsilon + n + 1)} \frac{(y/\varepsilon^s)^n}{(n + \sigma/\varepsilon)} \tag{2.10}$$

Hence for rectangles we have the solution

$$G_0^{(h)}(x, y, q) = \frac{1}{\varepsilon} \exp\left(\frac{\sigma\tau}{\varepsilon}\right) B_x\left(\frac{\sigma}{\varepsilon} + 1, 0\right) \tag{2.11}$$

where $B_x(a, b)$ is the incomplete beta function. For Ferrers diagrams the solution can be written in terms of the incomplete gamma function $\gamma(a, b)$ as

$$G_1^{(h)}(x, y, q) = \exp\left[\frac{y}{\varepsilon} - \frac{\sigma}{\varepsilon} \log\left(\frac{y}{\varepsilon}\right)\right] \gamma\left(\frac{\sigma}{\varepsilon} + 1, \frac{sy}{\varepsilon}\right) \tag{2.12}$$

The solution for stacks is expressible in terms of a less common hypergeometric function. For $q = 1$ one obtains the perimeter–generating functions

$$G_s^{(h)}(x, y, 1) = \frac{\sigma^{s-1} y}{\sigma^s - y} \tag{2.13}$$

One can also take the semicontinuous limit in the horizontal direction of the discrete solution (2.2) by

$$G_s^{(h)}(x, y, q) = \lim_{a \to 0} a^{1-s} G_s(x^a, a^s y, q^a) \tag{2.14}$$

which leads to the same solution.

On the other hand, in order to take the limit in the vertical direction, we write

$$G_s^{(v)}(x, y, q) = \lim_{a \to 0} G_s(ax, y^a, q^a) \qquad (2.15)$$

and taking this limit in (2.1) leads to the differential equation

$$\varepsilon x \frac{\partial}{\partial x} G_s^{(v)}(x, y, q) + \tau G_s^{(v)}(x, y, q) = x[1 + sG_s^{(v)}(x, y, q)] \qquad (2.16)$$

For $s = 1, 2$ the solution is given by an expression which again involves an incomplete gamma function

$$G_s^{(v)}(x, y, q) = \frac{1}{s} \exp\left[\frac{sx}{\varepsilon} - \frac{\tau}{\varepsilon} \log\left(\frac{sx}{\varepsilon}\right)\right] \gamma\left(\frac{\tau}{\varepsilon} + 1, \frac{sx}{\varepsilon}\right) \qquad (2.17)$$

Note the identity

$$G_2^{(v)}(x, y, q) = \tfrac{1}{2} G_1^{(v)}(2x, y, q) \qquad (2.18)$$

This arises because there is a mapping between the configuration of stacks and Ferrers diagrams in this limit. Briefly, one can build a stack of horizontal length n_x from a Ferrers diagram by starting with the tallest column of the Ferrers diagram and successively choosing to place the next largest column to either side of it. In this way one can construct $2^{n_x - 1}$ such stacks. In the vertical semicontinuous limit, configurations with columns of equal height are of measure zero and so there is an exact relation between the number of such stacks and Ferrers diagrams.

If one solves the differential equation (2.16) in the case $s = 0$ one gets the result $x/(\varepsilon + \tau)$, i.e., the generating function for just a single column. The correct vertical semicontinuous limit for rectangles is given as

$$G_0^{(v)}(x, y, q) = \lim_{a \to 0} aG_0(x, y^a, q^a) \qquad (2.19)$$

and leads to

$$\varepsilon x \frac{\partial}{\partial x} G_0^{(v)}(x, y, q) + \tau G_0^{(v)}(x, y, q) = \frac{x}{1 - x} \qquad (2.20)$$

Solving this equation results in an expression again involving an incomplete beta function

$$G_0^{(v)}(x, y, q) = \frac{1}{\varepsilon} x^{-\tau/\varepsilon} \int_0^x \frac{t^{\tau/\varepsilon} \, dt}{1 - t} \qquad (2.21)$$
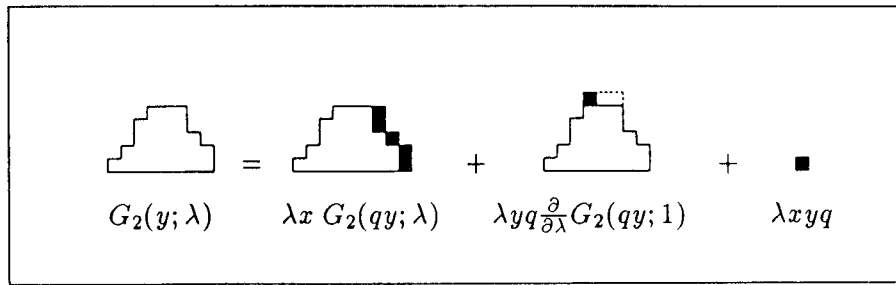
Fig. 4. An alternative functional equation for stacks.

Of course these results are expected since symmetry demands

$$G_{0,1}^{(v)}(x, y, q) = G_{0,1}^{(h)}(y, x, q) \tag{2.22}$$

However, for stacks the semicontinuous limits are different and we get two different generating functions. We will later demonstrate that the interesting asymptotic behaviors are the same for the two semicontinuous limits (as well as for the discrete model). To accomplish this we will need the differential equation satisfied by the horizontal semicontinuous stack solution. We can of course work backward and get a differential equation directly from (2.10), but there is also a direct derivation using functional equations. If we want to use horizontal instead of vertical inflation, we need to keep track of the top width of stacks by introducing an auxiliary variable λ conjugate to it, writing $G_2(x, y, q; \lambda)$ with $G_2(x, y, q) = G_2(x, y, q; 1)$. We can then use the inflation process to write (see Fig. 4)

$$G_2(x, y, q; \lambda) = \lambda x G_2(x, yq, q; \lambda) + \lambda yq \left(x + \frac{\partial}{\partial \lambda}\bigg|_{\lambda=1} G_2(x, y, q; \lambda) \right) \tag{2.23}$$

Denoting

$$H(x, y, q) = \frac{\partial}{\partial \lambda}\bigg|_{\lambda=1} G_2(x, y, q; \lambda) \tag{2.24}$$

we transform this to the equivalent system

$$G_2(x, y, q) = xG_2(x, yq, q) + yq[x + H(x, y, q)]$$
$$H(x, y, q) = G_2(x, y, q) + xH(x, yq, q) \tag{2.25}$$

This system can further be transformed to one functional equation in G_2 only, which can then be solved by standard techniques, leading to the already known result (2.2). Taking the semicontinuous limit horizontally in

this system leads to (note that differentiation with respect to λ introduces an additional factor of a)

$$\varepsilon y \frac{\partial}{\partial y} G_2^{(h)}(x, y, q) + \sigma G_2^{(h)}(x, y, q) = y[1 + H^{(h)}(x, y, q)]$$

$$\varepsilon y \frac{\partial}{\partial y} H^{(h)}(x, y, q) + \sigma H^{(h)}(x, y, q) = G_2^{(h)}(x, y, q)$$

(2.26)

This system now results in a linear *second*-order differential equation for $G_2^{(h)}$,

$$\left(\varepsilon y \frac{\partial}{\partial y} + \sigma\right) \frac{1}{y} \left(\varepsilon y \frac{\partial}{\partial y} + \sigma\right) G_2^{(h)}(x, y, q) = \sigma + G_2^{(h)}(x, y, q) \quad (2.27)$$

which is satisfied by the above solution (2.10), as one can readily check.

3. THE SINGULARITY STRUCTURE

Let us now consider the singularity structure of generating functions. First, we consider this singularity structure in the case of the discrete models (see Fig. 5).

Considering Eq. (2.2) as a power series in y, we see that its radius of convergence is given, for $0 < x \leqslant 1$, as

$$y_c(x, q) = \begin{cases} 1/q, & 0 < q < 1 \\ (1 - x)^s, & q = 1 \\ 0, & q > 1 \end{cases} \quad (3.1)$$

For both $q < 1$ and $q = 1$ the generating function has a simple pole at its radius of convergence. For $x > 1$ there is a divergence in the generating function at $q = 1/x$ and so, considering only $q < 1/x$, the radius of convergence is

$$y_c(x, q) = 1/q \quad \text{for} \quad 0 < q < 1/x \quad (3.2)$$

For $z = x = y$ this information reduces to

$$z_c(q) = \begin{cases} 1/q, & 0 < q < 1 \\ z_s, & q = 1 \\ 0, & q > 1 \end{cases} \quad \text{where} \quad z_s = \begin{cases} 1, & s = 0 \\ 1/2, & s = 1 \\ (3 - \sqrt{5})/2, & s = 2 \end{cases} \quad (3.3)$$

so we see a jump discontinuity at $q = 1$. For stacks and Ferrers diagrams we moreover have an isolated point $z_c(1) = z_s$. This is exactly the behavior
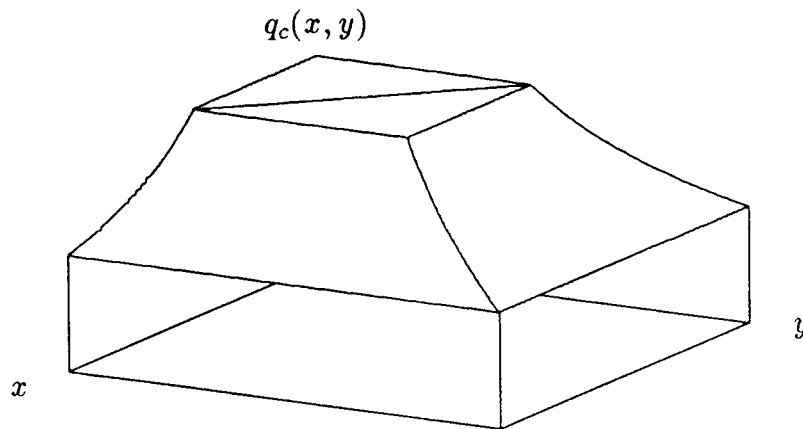
$$q_c(x, y)$$

Fig. 5. A schematic plot of the radius of convergence $q_c(x, y)$ of the generating function for the model of Ferrers diagrams. The square in the $q = 1$ plane is defined by the lines $x = 0, 1$ and $y = 0, 1$. The curved regions are defined by $q = 1/x$ and $q = 1/y$.

discussed in the Introduction and shown on the right-hand side of Fig. 2. There is a simple pole in the generating function at $q = 1$ for $s = 1, 2$ and a double pole for rectangles. For $q < 1$, there is a pole of order $s + 1$ at $z_c(q)$.

Returning to the full (x, y) plane, for $s = 1, 2$ we have a whole critical line

$$y = (1 - x)^s \tag{3.4}$$

at which the behavior of the generating function changes character. This line is also the radius of convergence of the perimeter-only generating function $G_s(x, y, 1)$ [see Eq. (2.8)], as we have catalogued above. The function $G_s(z, z, q)$ is the generating function of the fixed-perimeter partition functions $P_n(q)$, and the behavior detailed in (3.3) means that there is an isolated point in the perimeter free energy at $q = 1$.

A similar behavior can be extracted for the semicontinuous models. We consider the horizontal semicontinuous limit (the behavior for the other limit can be extracted from what is said here and the symmetry and functional relations between the two limits). Even though Eq. (2.10) is a power series in y, let us consider the locus of singularities in the variable x closest to the origin. For $0 < y < \infty$ this locus can be seen to be

$$x_c(y, q) = \begin{cases} 1/q, & 0 < q < 1 \\ \exp(-y^{1/s}), & q = 1 \\ 0, & q > 1 \end{cases} \tag{3.5}$$

when $s = 1, 2$. For $s = 0$ and given that $0 < y < 1$, the locus $x_c(y, q)$ has the same behavior as above for $0 < q < 1$ and $q > 1$ with $x_c(y, 1) = 1$. For fixed

y there is a pole in the generating function for both $q < 1$ and $q = 1$ in each of the models. Let us put $y = 1$ for the sake of comparison and let $z = x$. Now, we see that in a fashion mimicking the discrete model we have

$$z_c(q) = \begin{cases} 1/q, & 0 < q < 1 \\ z_s, & q = 1 \\ 0, & q > 1 \end{cases} \quad \text{where} \quad z_s = \begin{cases} 1, & s = 0 \\ 1/e, & s = 1 \\ 1/e, & s = 2 \end{cases} \tag{3.6}$$

Hence for stacks and Ferrers diagrams similar jumps in the radius of convergence occur in both the discrete models and these semicontinuous cases at $q = 1$.

Let us now consider the generating function of the fixed-area partition functions $A_m(x, y)$. Examining the generating function in this way, one finds that the area free energy is continuous. Precisely, the radius of convergence in q (and hence the free energy) as a function of x and y is given as

$$q_c(x, y) = \min\{1, 1/x, 1/y\} \tag{3.7}$$

for the discrete models (see Fig. 5) and

$$q_c(x, y) = \min\{1, 1/x\} \tag{3.8}$$

for the (horizontal) semicontinuous cases [for rectangles $q_c(x, y) = 0$ for $y > 1$]. In the discrete case there are only nonanalyticities at $(x = 1, y \leqslant 1)$, $(x \leqslant 1, y = 1)$, and at $x = y$ for $x, y > 1$. For the semicontinuous case there are only nonanalyticities at $x = 1$ (and also at $y = 1$ for rectangles). The significance of the line $y = (1 - x)^s$ $[x = \exp(-y^{1/s})]$ now is not that
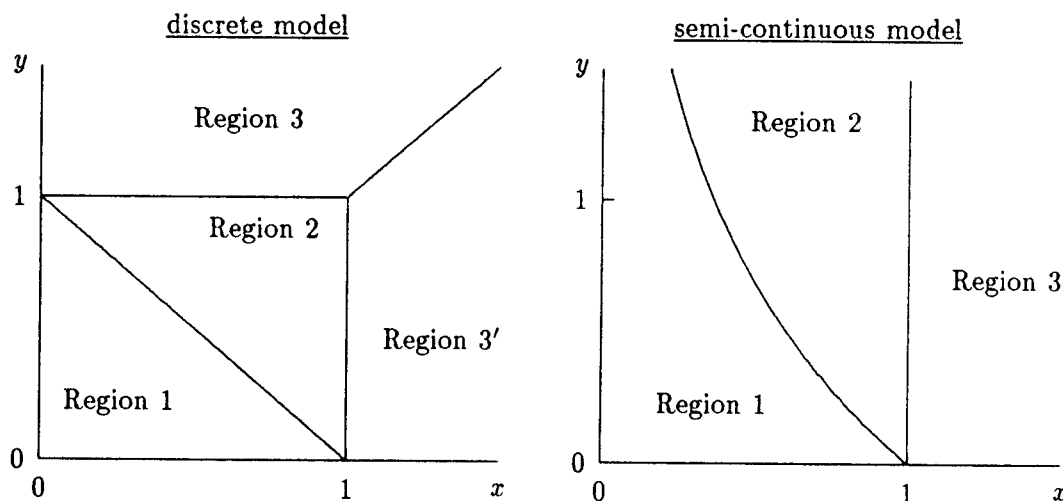

Fig. 6. The phase diagram in the x–y plane for the model of Ferrers diagrams. Stack polygons have a similar diagram (see text). The discrete case is shown on the left and the horizontal semicontinuous case on the right.

$q_c(x, y)$ exhibits a nonanalyticity, but rather that the generating function changes behavior on crossing this line from being finite at $q_c = 1$ to becoming infinite at $q_c = 1$ for the discrete (and semicontinuous) models.

The phase diagram for the discrete Ferrers diagrams is depicted on the left-hand side of Fig. 6. The critical line $y = 1 - x$ separating regions 1 and 2 transforms to the parabola $y = (1 - x)^2$ for stacks. This transition disappears for rectangles—here region 2 disappears completely. The phase diagram for the horizontal semicontinuous Ferrers diagrams is depicted on the right-hand side of Fig. 6. For rectangles there is again no region 2, and moreover there is a line at $y = 1$ heralding that the generating function has zero radius of convergence for $y \geqslant 1$.

We now discuss the asymptotic behavior of the generating as a function in q in more detail in the various regions of interest. We begin with the discrete models.

3.1. Discrete Models

3.1.1. Region 1.
In region 1, that is, for $y < (1 - x)^s$ (respectively $x, y < 1$ for rectangles), the generating function converges at $q_c = 1$ to the perimeter-only generating function. As $q_c = 1$ is an accumulation point of poles for fixed x and y, there has to be an essential singularity in q at $q_c = 1$.

3.1.2. Region 2.
This region is given by $y > (1 - x)^s$ and $x, y < 1$. Obviously it only exists for $s = 1, 2$. The generating function diverges, and we can compute the asymptotic behavior as $q \to 1$ by using (A.4) of the appendix to approximate the q-products. We get for $x < 1$

$$G_s(x, y, q) = \sum_{n=1}^{\infty} \frac{x(yq)^n}{1 - q^n x} \left(\frac{(q^n x; q)_\infty}{(qx; q)_\infty} \right)^s$$

$$\sim \sum_{n=1}^{\infty} \frac{x(yq)^n}{1 - q^n x} \left(\frac{1 - q^n x}{1 - qx} \right)^{s/2} e^{(s/\varepsilon)\{\mathrm{Li}_2(qx) - \mathrm{Li}_2(q^n x)\}}$$

$$\sim \int_0^\infty \frac{x(yq)^n}{1 - q^n x} \left(\frac{1 - q^n x}{1 - qx} \right)^{s/2} e^{(s/\varepsilon)\{\mathrm{Li}_2(qx) - \mathrm{Li}_2(q^n x)\}} \, dn$$

$$= \frac{x}{\varepsilon} (1 - qx)^{-s/2} e^{(s/\varepsilon) \mathrm{Li}_2(qx)} \int_0^1 (1 - tx)^{s/2 - 1}$$

$$\times e^{(1/\varepsilon)\{\tau \log t - s \mathrm{Li}_2(tx)\}} \, dt \tag{3.9}$$

The integral is of the form $\int e^{-\lambda g(t)} f(t) \, dt$ with $\lambda = 1/\varepsilon$ and

$$g(t) = -\tau \log t + s \mathrm{Li}_2(tx) \quad \text{and} \quad f(t) = (1 - tx)^{s/2 - 1} \tag{3.10}$$

There is a saddle point given by

$$g'(t_0) = 0 \rightarrow y = (1 - t_0 x)^s \rightarrow t_0 = \frac{1 - y^{1/s}}{x} \tag{3.11}$$

which is in $(0, 1)$ for $y > (1 - x)^s$. Hence we can use the saddle point approximation

$$\int e^{-\lambda g(t)} f(t) \, dt \sim \left[\frac{2\pi}{\lambda g''(t_0)} \right]^{1/2} f(t_0) \, e^{-\lambda g(t_0)} \tag{3.12}$$

We have

$$g''(t_0) = \frac{s x^2}{y^{1/s}(1 - y^{1/s})} \quad \text{and} \quad f(t_0) = y^{1/2 - 1/s} \tag{3.13}$$

Using a functional equation for the dilogarithm $\mathrm{Li}_2(x)$

$$\mathrm{Li}_2(x) + \mathrm{Li}_2(1 - x) + \log(x) \log(1 - x) - \frac{\pi^2}{6} = 0 \tag{3.14}$$

we can write

$$g(t_0) = -\sigma\tau + s \left(\frac{\pi^2}{6} - \mathrm{Li}_2(y^{1/s}) \right) \tag{3.15}$$

The prefactor of the integral simplifies for $q \approx 1$ to

$$\frac{x}{\varepsilon} (1 - qx)^{-s/2} \, e^{(s/\varepsilon) \, \mathrm{Li}_2(qx)} \sim \frac{x}{\varepsilon} (1 - x)^{s/2} \, e^{(s/\varepsilon) \, \mathrm{Li}_2(x)} \tag{3.16}$$

so that

$$G_s(x, y, q) \sim \left(\frac{2\pi}{s\varepsilon} \right)^{1/2} (1 - x)^{s/2} \left[(1 - y^{1/s}) \, y^{1 - 1/s} \right]^{1/2}$$

$$\times e^{\{(s/\varepsilon)[\mathrm{Li}_2(x) + \mathrm{Li}_2(y^{1/s}) + \log(x) \log(y^{1/s}) - \pi^2/6]\}} \tag{3.17}$$

as $\varepsilon \rightarrow 0$. We see that the prefactor gives trouble as $x \rightarrow 0$ or $y \rightarrow 1$. As the critical line $(y^{1/s} = 1 - x)$ is approached the exponentiated function vanishes [this can be seen with the help of (3.14)]. For completeness, we give explicitly

$$G_1(x, y, q) \sim \left(\frac{2\pi}{\varepsilon} \right)^{1/2} \left[(1 - x)(1 - y) \right]^{1/2}$$

$$\times e^{(1/\varepsilon)[\mathrm{Li}_2(x) + \mathrm{Li}_2(y) + \log(x) \log(y) - \pi^2/6]} \tag{3.18}$$

and

$$G_2(x, y, q) \sim \left(\frac{\pi}{\varepsilon}\right)^{1/2} (1-x)[\sqrt{y}(1-\sqrt{y})]^{1/2}$$

$$\times e^{(2/\varepsilon)[\,\mathrm{Li}_2(x)\,+\,\mathrm{Li}_2(\sqrt{y})\,+\,\log(x)\,\log(\sqrt{y})\,-\,\pi^2/6\,]} \tag{3.19}$$

3.1.3. Critical Line Separating Regions 1 and 2. The critical line is given as $y = (1-x)^s$ for $s = 1, 2$. We can repeat the calculation from the previous section, with the only difference being that the saddle point $t_0 = 1$ is now at the boundary of the integration. This means that we only pick up half a Gaussian integral. As mentioned in the previous section, the exponential part vanishes on the critical line and we get

$$G_s(x, y, q) \sim \left(\frac{\pi}{2s\varepsilon}\right)^{1/2} (1-x)^{s/2} \left[(1-y^{1/s})\, y^{1-1/s}\right]^{1/2} \tag{3.20}$$

3.1.4. Critical Lines Separating Regions 2 and 3, and 2 and 3'. Let us first consider the asymptotics for $y = 1$. Again we can use the above calculation, leading to

$$G_s(x, 1, q) \sim \frac{x}{\varepsilon} (1-qx)^{-s/2}\, e^{(s/\varepsilon)\,\mathrm{Li}_2(qx)} \int_0^1 (1-tx)^{s/2-1}$$

$$\times e^{-(s/\varepsilon)\,\mathrm{Li}_2(tx)}\, dt \tag{3.21}$$

For $s = 1, 2$ we notice that the exponential part $g(t) = s\,\mathrm{Li}_2(tx)$ has its minimum at $t_0 = 0$, that is, the integral boundary with $g'(t) = sx$. Therefore we have

$$G_s(x, 1, q) \sim \frac{1}{s} (1-x)^{s/2}\, e^{(s/\varepsilon)\,\mathrm{Li}_2(x)} \tag{3.22}$$

For rectangles on the other hand, where $y = 1$ separates regions 1 and 3, (3.21) gives directly

$$G_0(x, 1, q) \sim -\frac{1}{\varepsilon} \log(1-x) \tag{3.23}$$

Identical formulas hold for $x = 1$ for rectangles and Ferrers diagrams due to their symmetry. However, for stacks we have to work a bit harder. We start again with the series representation of the generating function, but now we insert (A.11) to get

$$G_s(1, y, q) = \sum_{n=1}^{\infty} \frac{(yq)^n}{1-q^n} \left(\frac{(q^n; q)_\infty}{(q; q)_\infty} \right)^s$$

$$\sim \sum_{n=1}^{\infty} \frac{(yq)^n}{1-q^n} \left(\frac{I(n)}{I(1)} \right)^s \left(\frac{1-q^n}{1-q} \right)^{s/2} e^{(s/\varepsilon)\{\text{Li}_2(q) - \text{Li}_2(q^n)\}}$$

$$\sim \int_0^\infty \frac{(yq)^n}{1-q^n} \left(\frac{I(n)}{\sqrt{2\pi/e}} \right)^s \left(\frac{1-q^n}{1-q} \right)^{s/2} e^{(s/\varepsilon)\{\text{Li}_2(q) - \text{Li}_2(q^n)\}} \, dn$$

$$= \frac{1}{\varepsilon} \left(\frac{e}{\sqrt{2\pi}} \right)^s (1-q)^{-s/2} e^{(s/\varepsilon)\,\text{Li}_2(q)} \int_0^1 \left[I \left(\frac{-\log(t)}{\varepsilon} \right) \right]^s (1-t)^{s/2-1}$$

$$\times e^{(1/\varepsilon)\{\tau \log t - s\,\text{Li}_2(t)\}} \, dt \tag{3.24}$$

Except for the factor $[I(-\log(t)/\varepsilon)]^s$, the integral is identical to the one dealt with above. Moreover, we have

$$I(r) = 1 + O(1/r) \qquad \text{as} \qquad r \to \infty \tag{3.25}$$

As the saddle point $t_0 = 1 - y^{1/s}$ is less than one, we can continue to write

$$G_s(1, y, q) \sim \left(\frac{s}{2\pi} \right)^{(s-1)/2} [y^{1-1/s}(1 - y^{1/s})]^{1/2} e^{(s/\varepsilon)\,\text{Li}_2(y^{1/s})} \tag{3.26}$$

For $s = 1$ we recover the above result, and for $s = 2$ we get

$$G_2(1, y, q) \sim \frac{1}{\sqrt{\pi}} [\sqrt{y}(1 - \sqrt{y})]^{1/2} e^{(2/\varepsilon)\,\text{Li}_2(\sqrt{y})} \tag{3.27}$$

Note that in the case of Ferrers diagrams the calculations would have been considerably abbreviated, since we could have evaluated the identity (2.5). However, no such identity is for available stacks.

3.1.5. Critical Point Separating Regions 2, 3, and 3'. In the case $x = 1$ and $y = 1$, we can also utilize the calculation from the previous section for $s = 1, 2$. We get, after a few steps,

$$G_s(1, 1, q) \sim \frac{1}{s} \left(\frac{\varepsilon}{2\pi} \right)^{s/2} e^{(s/\varepsilon)\,\pi^2/6} \tag{3.28}$$

Alternatively, we could have used the explicit formulas (2.5) and (2.6). For rectangles, the point $x = 1$ and $y = 1$ separates regions 1, 3, and 3' and we get

$$G_0(1, 1, q) \sim \frac{1}{\varepsilon} \log \left(\frac{1}{\varepsilon} \right) \tag{3.29}$$

3.1.6. Regions 3 and 3'. We rewrite (2.2) as

$$G_s(x, y, q) = \frac{xyq}{1 - xq} + \frac{1}{(1 - xq)^s} \sum_{n=1}^{\infty} \frac{x(yq)^{n+1}}{(xq^2; q)_{n-1}^s (1 - xq^{n+1})} \qquad (3.30)$$

In region 3', where $x > 1$ with $x > y$, we therefore get as $q \to 1/x$

$$G_s(x, y, q) \sim \begin{cases} \dfrac{y}{1 - xq}, & s = 0 \\[3mm] \dfrac{y}{1 - xq} \dfrac{1}{(y/x; 1/x)_\infty}, & s = 1 \\[3mm] \dfrac{y}{(1 - xq)^2} \displaystyle\sum_{n=1}^{\infty} \dfrac{(y/x)^n}{(1/x; 1/x)_{n-1}(1/x; 1/x)_n}, & s = 2 \end{cases} \qquad (3.31)$$

For $s = 0, 1$, these results can be transferred to region 3 as well. For stacks, however, we have to argue differently; interpreting (2.2) as a series expansion in $t = yq$, we see that for $q = 1/y$ the coefficients of the series approach $x/(x/y; 1/y)_\infty^s$ as $n \to \infty$. Therefore, we have the asymptotic behavior for $q \to 1/y$ given as

$$G_s(x, y, q) \sim \frac{x}{1 - yq} \frac{1}{(x/y; 1/y)_\infty^s} \qquad (3.32)$$

This matches with the above calculation for $s = 0, 1$ and gives the desired result for stacks.

3.1.7. Critical Line Separating Regions 3 and 3'. For $x = y > 1$, we write, as above,

$$G_s(x, x, q) = \frac{x^2 q}{1 - xq} + \frac{1}{(1 - xq)^s} \sum_{n=1}^{\infty} \frac{x(xq)^{n+1}}{(xq^2; q)_{n-1}^s (1 - xq^{n+1})} \qquad (3.33)$$

and now use the transformation $t = xq$ and $p = 1/x < 1$ to write

$$\frac{1}{x} G_s(x, x, q) = \frac{t}{1 - t} + \frac{t}{(1 - t)^s} \sum_{n=1}^{\infty} \frac{t^n}{(t^2 p; tp)_{n-1}^s [1 - t(tp)^n]} \qquad (3.34)$$

For p fixed and $t \to 1$, the first term diverges with a simple pole, whereas the sum diverges as

$$\frac{1}{(1 - t)^{s+1}} \frac{1}{(p; p)_\infty^s} \qquad (3.35)$$

Therefore, we have

$$
G_s(x, x, q) \sim
\begin{cases}
\dfrac{2x}{1-xq}, & s=0 \\[2ex]
\dfrac{x}{(1-xq)^2} \dfrac{1}{(1/x; 1/x)_\infty}, & s=1 \\[2ex]
\dfrac{x}{(1-xq)^3} \dfrac{1}{(1/x; 1/x)_\infty^2}, & s=2
\end{cases}
\tag{3.36}
$$

3.2. Semicontinuous Models

3.2.1. Ferrers Diagrams and Stacks.

Although we have discussed the asymptotic behavior of the discrete generating functions in detail, we have not yet described the crossover between the different regions, let alone calculated any scaling functions describing this crossover. We shall do this now from the semicontinuous model. First, however, let us note that the semicontinuous limit produces only a restricted phase diagram, as either region 3′ or region 3 gets scaled away to infinity (see Fig. 6). Under the vertical limit, the critical line $y = (1-x)^s$ gets transformed to $\tau = sx$, whereas under the horizontal limit, we get $y = \sigma^s$.

To begin we examine the horizontal semicontinuous limit for Ferrers diagrams. From the full solution

$$
G_1^{(h)}(x, y, q) = \exp\left[\frac{y}{\varepsilon} - \frac{\sigma}{\varepsilon} \log\left(\frac{y}{\varepsilon}\right) \right] \gamma\left(\frac{\sigma}{\varepsilon} + 1, \frac{y}{\varepsilon}\right)
\tag{3.37}
$$

we can extract most of the necessary information. However, we are most interested in the behavior for small ε near the boundary of region 1 and region 2. First, we note that the behavior for small ε in regions 1, 2, and 3 (and the boundaries) is the same in this limit as for the discrete models. It is not too difficult to extract asymptotic formulas of the same forms (in ε) as Eqs. (3.20), (3.17), (3.26), and (3.31). (Note that the resulting formulas are only the same in the variable ε.) All this means is that if one fixes $y < 1$ in either the discrete or the horizontal semicontinuous models one obtains the same phase diagram and critical behavior in the (x, q) plane. (Similarly for $x < 1$ and the vertical semicontinuous model.) Now that we have ascertained this, we can use the semicontinuous model to find more easily the scaling function around the boundary of region 1 and region 2.

Rather than use the solution itself, it is easier to work with the differential equation (2.16). Note that because of the relations (2.22) and (2.18), this also gives us the asymptotics of the vertical semicontinuous stacks and Ferrers diagrams. Denoting $g(x) = G_1^{(h)}(x, y, q)$, we have

$$\varepsilon x g'(x) = (x - \sigma) g(x) + x \qquad (3.38)$$

from which we can get the crossover behavior by following ref. 10. We first transform the critical point to the origin,

$$-\varepsilon(t + \sigma)/p'(t) = stp(t) + (t + \sigma) p^2(t) \qquad \text{where} \quad p(t) = 1/g(t + \sigma) \qquad (3.39)$$

Substituting $p = \varepsilon^\theta \bar{p}$ and $t = \varepsilon^\phi \bar{t}$, we now look for the dominating terms in this equation for $\varepsilon \to 0$. This yields $\theta = \phi = 1/2$, and we get a differential equation for the asymptotically dominant part as

$$-\sigma \bar{p}'(\bar{t}) = \bar{t}\bar{p}(\bar{t}) + \sigma \bar{p}^2(\bar{t}) \qquad (3.40)$$

Solving this equation and fixing the arbitrary constant by using asymptotic matching with the solution for $\varepsilon = 0$ results in the scaling solution

$$G_1^{(h)}(x, y, q) \sim \left(\frac{\pi\sigma}{2\varepsilon}\right)^{1/2} \exp\left(\frac{(\sigma - y)^2}{2\varepsilon\sigma}\right) \mathrm{erfc}\left(\frac{\sigma - y}{(2\varepsilon\sigma)^{1/2}}\right) \qquad (3.41)$$

From this we can easily read off the whole crossover behavior as $\sigma - y$ changes sign. Note that for $\sigma = y$ one obtains the same form as (3.20). The scaling variable is $(\sigma - y)/\sqrt{\varepsilon}$. Moreover, since

$$G^{(h)}(x, y, q) = \int_0^\infty e^{-m\varepsilon} A_m(x, y) \, dm \qquad (3.42)$$

a direct inverse Laplace transform of the r.h.s. of Eq. (3.41) gives the scaling behavior of the area partition function as

$$A_m(x, y) \sim \left(\frac{\sigma}{2m}\right)^{1/2} \exp\left[(y - \sigma)\left(\frac{2m}{\sigma}\right)^{1/2}\right] \qquad (3.43)$$

This gives us the form of the behavior of A_m in region 1 as described in Eq. (1.12) when $\sigma > y$.

The scaling behavior around the transition at $\sigma = 0$ between regions 2 and 3 can be read off from the full station. The incomplete gamma function simplifies and one gets

$$G_1^{(h)}(x, y, q) \sim \exp(y/\varepsilon)(y/\varepsilon)^{-\lambda} \Gamma(\lambda + 1) \qquad (3.44)$$

where $\lambda = \sigma/\varepsilon$ and we see a crossover from an essential singularity in $\varepsilon \to 0$ for $\sigma > 0$ to a simple pole at $\varepsilon = -\sigma$ for $\sigma < 0$. However, this expression cannot be written as a crossover scaling form, even though the natural scaling variable $\lambda = \sigma/\varepsilon$ nearly works. Note that this gives the form (3.26) for $\sigma = 0$.

The other case to consider is the horizontal semicontinuous limit of the stack model. The full solution is not simply related to the incomplete gamma function as is the vertical limit. However, here we illustrate that it is dominated by a scaling solution around the line separating regions 1 and 2 [now this is $(y = \sigma^2, \varepsilon)$] similar to the one described above. The differential equation (2.27), in the variable y, can be expanded to

$$\varepsilon^2 g''(y) + 2\varepsilon\sigma g'(y) + [\sigma(\sigma - \varepsilon)/y - 1] g(y) = \sigma \qquad (3.45)$$

where $g(y) = G_2^{(h)}(x, y, q)$. The critical point is given by the point at which the prefactor of $g(y)$ is equal to 0. We first transform the critical point to the origin,

$$\varepsilon^2(\sigma^2 + t^2)[2(p')^2 - p''p] - 2\varepsilon\sigma(\sigma^2 + t) \, p'p - (\sigma\varepsilon) \, p^2$$

$$= \sigma(\sigma^2 + t) \, p \qquad \text{where} \quad p(t) = \frac{1}{g(t + \sigma^2)} \qquad (3.46)$$

Substituting $p = \varepsilon^\theta \bar{p}$ and $t = \varepsilon^\phi \bar{t}$, we now look for the dominating terms in this equation for $\varepsilon \to 0$. This yields $\theta = \phi = 1/2$, and we get a differential equation for the asymptotically dominant part as

$$-2\sigma^3 \bar{p}'(\bar{t}) = \bar{t}\bar{p}(\bar{t}) + \sigma^3 \bar{p}^2(\bar{t}) \qquad (3.47)$$

Solving this equation and fixing the arbitrary constant by using asymptotic matching with the solution for $\varepsilon = 0$ results in the scaling solution

$$G_2^{(h)}(x, y, q) \sim \frac{1}{2}\left(\frac{\pi\sigma^3}{\varepsilon}\right)^{1/2} \exp\left(\frac{(\sigma^2 - y)^2}{4\varepsilon\sigma^3}\right) \text{erfc}\left(\frac{\sigma^2 - y}{2(\varepsilon\sigma^2)^{1/2}}\right) \qquad (3.48)$$

One can compare this to the scaling solution for the vertical limit, which is

$$G_2^{(v)}(x, y, q) \sim \frac{1}{2}\left(\frac{\pi\tau}{2\varepsilon}\right)^{1/2} \exp\left(\frac{(\tau - 2x)^2}{2\varepsilon\tau}\right) \text{erfc}\left(\frac{\tau - 2x}{(2\varepsilon\tau)^{1/2}}\right) \qquad (3.49)$$

This demonstrates the universality of the models: the scaling functions are the same, though the nonuniversal constants differ. The "near-scaling" around $\sigma = 0$ for $G_2^{(v)}(x, y, q)$ can be easily seen to be essentially the same as that described above for Ferrers diagrams [see Eq. (3.44)] using (2.18).

3.2.2. Rectangles. The semicontinuous limit for rectangles has a different phase diagram. There is a natural boundary at $y = 1$, so that the radius of convergence is 0 for $y \geqslant 1$. In common with the discrete model, it does not contain a region 2. For the horizontal semicontinuous case the boundary of the regions 1 and 3 is $x = 1$. The solution

$$G_0^{(h)}(x, y, q) = \sum_{n=1}^{\infty} \frac{y^n}{\sigma + n\varepsilon} \tag{3.50}$$

is easily analyzed. The behavior is exactly the same in the variable ε for fixed x and y: that is, region 3 has a simple pole at $\varepsilon = \sigma$ [see (3.31)], region 1 has a convergent essential singularity, and the boundary has a simple pole [see (3.23)]. Also, the perimeter generating function has a simple pole at $x = 1$ for $y < 1$. Of some interest, perhaps, is that the generating function can be written in a scaling form in the variable $\lambda = \sigma/\varepsilon$ around the boundary of regions 1 and 3:

$$\varepsilon G_0^{(h)}(x, y, q) = \sum_{n=1}^{\infty} \frac{y^n}{\lambda + n} \tag{3.51}$$

Hence, the scaling function is a Lerch function.

APPENDIX

q-Product Asymptotics

Here, we discuss the asymptotics for q-products as $q \to 1$. As the full asymptotics of q-products has been discussed elsewhere,[19] we are rather brief in doing so. For $0 < q < 1$ and $0 < t < 1$, we are interested in the asymptotics of $(t; q)_\infty$ and $(q; q)_\infty$ as $\varepsilon = -\log q \to 0$. In this range of parameters the elegant Abel–Plana formula[20] applies, and we can write

$$\log(t; q)_\infty = \int_0^\infty \log(1 - te^{-\varepsilon x}) \, dx + \frac{1}{2} \log(1 - t)$$

$$+ i \int_0^\infty \frac{\log(1 - te^{-i\varepsilon y}) - \log(1 - te^{i\varepsilon y})}{e^{2\pi y} - 1} \, dy$$

$$= -\frac{1}{\varepsilon} \mathrm{Li}_2(t) + \frac{1}{2} \log(1 - t) - 2 \int_0^\infty \frac{dy}{e^{2\pi y} - 1}$$

$$\times \arctan\left(\frac{t \sin \varepsilon y}{1 - t \cos \varepsilon y}\right) \tag{A.1}$$

The remaining effort lies in estimating the integral in the above formula. For $t < 1$, we see that

$$\left| \arctan \left(\frac{t \sin \varepsilon y}{1 - t \cos \varepsilon y} \right) \right| \leqslant \frac{t y \varepsilon}{1 - t} \tag{A.2}$$

so that the integral of this expression is $O(\varepsilon)$. Therefore we can write

$$\log(t; q)_\infty = -\frac{1}{\varepsilon} \operatorname{Li}_2(t) + \frac{1}{2} \log(1 - t) + O(\varepsilon) \tag{A.3}$$

and we have as our first result

$$(t; q)_\infty \sim (1 - t)^{1/2} e^{-\operatorname{Li}_2(t)/\varepsilon} \tag{A.4}$$

On the other hand, if we set $t = q$, then the integral contributes as well. We then have

$$\left| \arctan \left(\frac{q \sin \varepsilon y}{1 - q \cos \varepsilon y} \right) - \arctan(y) \right| \leqslant \frac{1}{2} y \varepsilon \tag{A.5}$$

and

$$\int_0^\infty \frac{dy}{e^{2\pi y} - 1} \arctan(y) = \frac{1}{4} \log(2\pi) - \frac{1}{2} \tag{A.6}$$

Therefore, to leading order we obtain

$$\log(q; q)_\infty = -\frac{1}{\varepsilon} \operatorname{Li}_2(q) + \frac{1}{2} \log(1 - q) + 1 - \frac{1}{2} \log(2\pi) + O(\varepsilon)$$

$$= -\frac{1}{\varepsilon} \frac{\pi^2}{6} + \frac{1}{2} \log \frac{2\pi}{\varepsilon} + O(\varepsilon) \tag{A.7}$$

so that now

$$(q; q)_\infty \sim (2\pi/\varepsilon)^{1/2} e^{-\pi^2/6\varepsilon} \tag{A.8}$$

Here, we could also have followed Hardy and used a conjugate-modulus transformation or $(q; q)_\infty$ to get a convergent expansion with the same leading term.[21]

Finally, we need the asymptotics for $(q^n; q)_\infty$ uniformly in n. We can easily generalize the previous estimate by writing

$$\left| \arctan \left(\frac{q \sin \varepsilon y}{1 - q^n \cos \varepsilon y} \right) - \arctan \left(\frac{y}{n} \right) \right| \leqslant \frac{1}{2} y \varepsilon \tag{A.9}$$

and so it turns out that the integral needed is the remainder term in the Stirling formula,

$$2 \int_0^\infty \frac{dy}{e^{2\pi y} - 1} \arctan\left(\frac{y}{n}\right) = \log \Gamma(n) - \left(n - \frac{1}{2}\right) \log n + n - \frac{1}{2} \log 2\pi \quad \text{(A.10)}$$

We get

$$(q^n; q)_\infty \sim I(n)(1 - q^n)^{1/2} e^{-\text{Li}_2(q^n)/\varepsilon} \quad \text{(A.11)}$$

with

$$I(n) = \frac{n^n e^{-n} (2\pi/n)^{1/2}}{\Gamma(n)} \quad \text{(A.12)}$$

ACKNOWLEDGMENTS

REFERENCES

1. H. N. V. Temperly, *Proc. Camb. Phil. Soc.* **48**:638 (1952).
2. L. Euler, *Introductio in Analysis Infinitorum* (Marcum-Michaelem Bousquet, Lausanne, 1748).
3. G. E. Andrews, in *The Theory of Partitions*, G.-C. Rota, ed. (Addison-Wesley, Reading, Massachusetts, 1976).
4. M. Delest and G. Viennot, *Theor. Comp. Sci.* **34**:169 (1984).
5. M. Delest, *J. Math. Chem.* **8**:3 (1991).
6. V. Privman and N. M. Švrakić, *Phys. Rev. Lett.* **60**:1107 (1988).
7. V. Privman and N. M. Švrakić, *Directed Models of Polymers, Interfaces, and Clusters: Scaling and Finite-Size Properties*, (Springer-Verlag, Berlin, 1989).
8. M. E. Fisher, A. J. Guttmann, and S. Whittington, *J. Phys. A* **24**:3095 (1991).
9. R. Brak, A. L. Owczarek, and T. Prellberg, *J. Stat. Phys.* **76**:1101 (1994).
10. T. Prellberg and R. Brak, *J. Stat. Phys.* **78**:701 (1995).
11. M. Bousquet-Mélou, A method for the enumeration of various classes of column-convex polygons, University of Bordeaux Preprint (1993).
12. M. Bousquet-Mélou, The generating function of convex polyominoes: the resolution of a q-differential system, University of Bordeaux Preprint (1993).
13. T. Prellberg and A. L. Owczarek, Partially convex lattice vesicles: Methods and recent results, *Int. J. Mod. Phys. B*, to appear.
14. G. H. Hardy and S. Ramanujan, *Proc. Lond. Math. Soc. (2)* **17**:75 (1918).

15. F. C. Auluck, *Proc. Camb. Phil. Soc.* **47**:679 (1951).
16. E. M. Wright, *Q. J. Math. Oxford (2)* **19**:313 (1968).
17. J. M. Fédou, *Rep. Math. Phys.* **34**:57 (1994).
18. A. L. Owczarek and T. Prellberg, *J. Stat. Phys.* **70**:1175 (1993).
19. T. Prellberg, Uniform q-series asymptotics for staircase polygons, *J. Phys. A* **28**:1289 (1995).
20. G. H. Hardy, *Divergent Series* (Oxford University Press, Oxford, 1963).
21. G. H. Hardy, *Ramanujan: Twelve Lectures on Subjects Suggested by His Life and Work* (Cambridge University Press, Cambridge, 1940).